Frontotemporal Dementia Linked to Chromosome 3 in *Saccharomyces cerevisiae*

by

Niles Sulkko

University of Colorado at Boulder

Department of Molecular, Cellular, and Developmental Biology

April 2013

Thesis Advisor:

Dr. Greg Odorizzi, Department of Molecular, Cellular, and Developmental Biology

Defense Committee:

Dr. Jennifer Martin, Department of Molecular, Cellular, and Developmental Biology

Dr. Christopher Link, Department of Integrative Physiology

Abstract

Frontotemporal dementia (FTD) represents a crippling new neurodegenerative disease for scientific investigation. Marked by characteristic frontal and temporal lobar cortical atrophy, FTD results in the progressive deterioration of social and behavioral capabilities. FTD exhibits an autosomal dominant inheritance pattern, and is the second most common form of presenile dementia behind Alzheimer's disease. One subtype of the neuropathy, designated as frontotemporal dementia linked to chromosome 3 (FTD3), has been traced to a single truncating mutation in the human protein CHMP2B. Fortunately, *S. cerevisiae* ortholog Vps2 shares conserved function with CHMP2B, and functions analogously as a constituent of the ESCRT-mediated endocytic pathway, necessary for protein trafficking and degradation within the cell. In order to investigate the mechanism and genetics behind FTD3 pathology, a corresponding mutation has been created in yeast, and a variety of assays examining its function have been conducted. This projects details the mutation's potential effects on autophagy, as well as the critical polymerization of ESCRT-III component Snf7. Ultimately, this exposition suggests that autophagy is not affected by the FTD3 mutation. Additionally, heterozygous expression of mutated Vps2 does not appear to cause aberrant Snf7 polymerization, while haploid expression does seem to affect the process. Finally, proposed future experiments should continue to help resolve the mechanism behind frontotemporal dementia linked to chromosome 3.

Introduction

A Clinical Presentation of FTD

Recent advancements in genetic testing and pedigree analysis have revealed a new type of debilitating neurodegenerative disease: frontotemporal dementia. Frontotemporal dementia,

known colloquially as FTD, exhibits an average age of onset in the late fifties, and is attributed to 20% of all dementia cases before the age of 65 (Skibinski et al., 2005). As a result, FTD represents the second most common cause of presenile dementia, behind Alzheimer's disease (Urwin et al., 2009). While all cases of FTD share the common characteristics of marked frontal and temporal lobar atrophy of the cerebral cortex, a variety of clinical symptoms are ascribed to specific categories of FTD. The most common designation, representative of 60% of FTD cases, is categorized as behavioral variant FTD (bvFTD) (Wittenberg et al., 2008). The hallmarks of bvFTD include distinct behavioral and emotional changes strikingly inconsistent with the patient's prior personality; apathy, disinhibition, impaired reasoning capacity, and a severe decrease in social abilities are all symptoms of bvFTD. In addition to bvFTD, two additional categories of FTD, characterized by pronounced language dysfunction, correspond to approximately 40% of all FTD cases. Progressive non-fluent aphasia (PNFA) FTD is categorized as FTD cases with severe impairment in speech production, yet intact comprehension of the meaning of words. In contrast, semantic dementia FTD results in deficits both in speech production and comprehension. In both cases, the progression of the disease often times decreases the capacity for empathy in patients, while additionally accompanied by the social and personality deficits observed in bvFTD (Hodges, 2001). Ultimately, cases of bvFTD and semantic FTD exhibit high rates of comorbidity in their diagnosis. The prognosis for all categories of FTD remains one marked by rapid onset followed by a steady neurological decline for 2-10 years before death.

Genetics of FTD

New and ongoing investigations into the underlying genetic basis for frontotemporal dementia have made progress in elucidating the cause of the disease. Approximately 40% of FTD cases are familial, and the condition is inherited in an autosomal dominant pattern (Seelaar et al., 2011). Consequently, an afflicted parent presents a 50% probability in passing the genetic mutation to their progeny. The most common mutations implicated in FTD heredity are localized to two genes along the long arm of chromosome 17. Mutations occurring in the MAPT (microtubule-associated protein tau) loci result in a designation of frontotemporal subclass FTDP-17T (Talbot & Ansorge, 2006). Responsible for an estimated 10% of all FTD cases, mutations in the MAPT genes on chromosome 17 produce the detrimental aggregation of tau protein in neurons, ultimately resulting in neuronal degradation. Similar to many types of neurodegenerative disease, FTDP-17T is classified as having a clear pathology in relation to the protein tau, known as a "taupathy". Comprising another approximate 10% of all FTD occurrences are those associated with null mutations in the PGRN (progranulin) gene, situated 1.7Mb upstream of the MAPT loci (Snowden et al., 2006). PGRN, among its many putative roles, serves as a neuronal growth and viability factor. Unlike FTDP-17T, PGRN-associated FTD results in tau-negative, ubiquitin-positive inclusions in the afflicted neurons. Ultimately, PGRN cases are thought to be the result of haploinsufficiency, with the mutations in the gene resulting in "premature mRNA truncation and nonsense mediated decay" (Mackenzie et al., 2006).

While the majority of FTD cases characterized thus far result from mutations in chromosome 17, a fascinating population has emerged linked to a single unique mutation on chromosome 3 (Van der Zee et al., 2008). First discovered in 1995 in the Jutland region of the

Netherlands, the pedigree of frontotemporal dementia linked to chromosome 3 (FTD3) spans 450 members and can be linked across six generations of a single Danish family (Skibinski et al., 2005). FTD3 is similar to PGRN-linked FTD in that both are tau-negative disease states with ubiquitinated inclusions (Talbot & Ansorge, 2006). However, unlike the majority of FTD cases where the primary ubiquitinated protein has been ascertained as TAR-binding protein 43 (TDP-43), FTD3 shows no such similarities, and is subsequently classified as a TDP-43-negative variant of FTD (Filimonenko et al., 2007). Ultimately, it is the single, unambiguous mutation in FTD3 which provides an intriguing problem for study. FTD3 arises from a single point mutation in the protein CHMP2B (charged multivesicular body protein 2B) resulting in a marked guanine to cytosine transition in the acceptor splice site of exon 6 (Isaacs et al., 2011). As a consequence, two aberrant transcripts are produced, both exhibiting a truncation of 36 amino acids in the carboxyl terminus of CHMP2B (Urwin et al., 2009). The first, designated as CHMP2B^intron5, creates a novel valine amino acid residue followed by a stop codon (Figure 1). The second resulting transcript produces a frame-shift mutation, the result of which produces 29 amino acids of a non-functional nonsense sequence.

Fortunately, CHMP2B in humans shares an exact ortholog in yeast: vacuolar protein sorting gene, or Vps2. As such, the model organism *Saccharomyces cerevisiae* can be implemented as an effective functional disease model for investigation into the genetics and molecular mechanisms responsible for FTD3. *S. cerevisiae* presents a relatively easily manipulated genome, as well as the ability to exist in either a haploid or diploid form, a trait which allows for excellent genotype experimentation and analysis. In relation to cell biology, orthologous proteins CHMP2B and Vps2 perform known critical roles in endosomal membrane

trafficking. Both function in their respective organisms as a component protein in the assembly of the heteromeric protein complex ESCRTIII (Endosomal Sorting Complex Required for Transport-III), the third and final of the ESCRT complexes necessary for protein degradation, recycling, and endosome trafficking within the cell. In order to understand the putative disease mechanisms behind FTD3, the endocytic pathway and its function as facilitated by the ESCRTs must be examined.

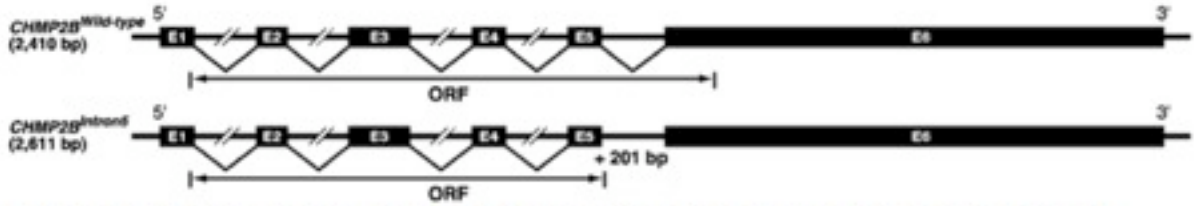

Figure 1: Schematic of both wild-type and aberrant CHMP2BΔFTD3 (CHMP2B^Intron5) transcripts. Mutant CHMP2B results in the premature truncation of 36 amino acids, and is the cause of frontotemporal dementia linked to chromosome 3 (FTD3). Figure from Urwin et al. 2009.

The Endocytic Pathway and Critical ESCRTs

The endocytic pathway represents an indispensable process in the trafficking and regulation of proteins away from the cell membrane and cytosol. This highly dynamic mechanism allows for the correct localization of cellular proteins to the endosome, where they are resigned to two potential fates. After initial budding into the early endosome, some proteins are recycled back to their area of function, often times back to the plasma membrane or golgi. This is often times the case for house-keeping receptors such as transferrin receptor, necessary for the maintenance of normal cell function (Russell et al., 2006). For other proteins, such as epidermal growth factor receptor (EGFR), uptake into the early endosome is the first step towards their ultimate degradation in the lysosome. As the early endosome matures to a late endosome, proteins targeted for degradation are facilitated into intraluminal vesicles (ILVs)

within the late endosome, creating a multivesicular body (MVB) (Raiborg & Stenmark, 2009). This progressive process is accompanied by both a change in membrane composition of the MVB and an increasingly acidic environment within the vesicle. Upon reaching its destination, the MVB finally fuses with the lysosome, resulting in the degradation of its lumenal contents.

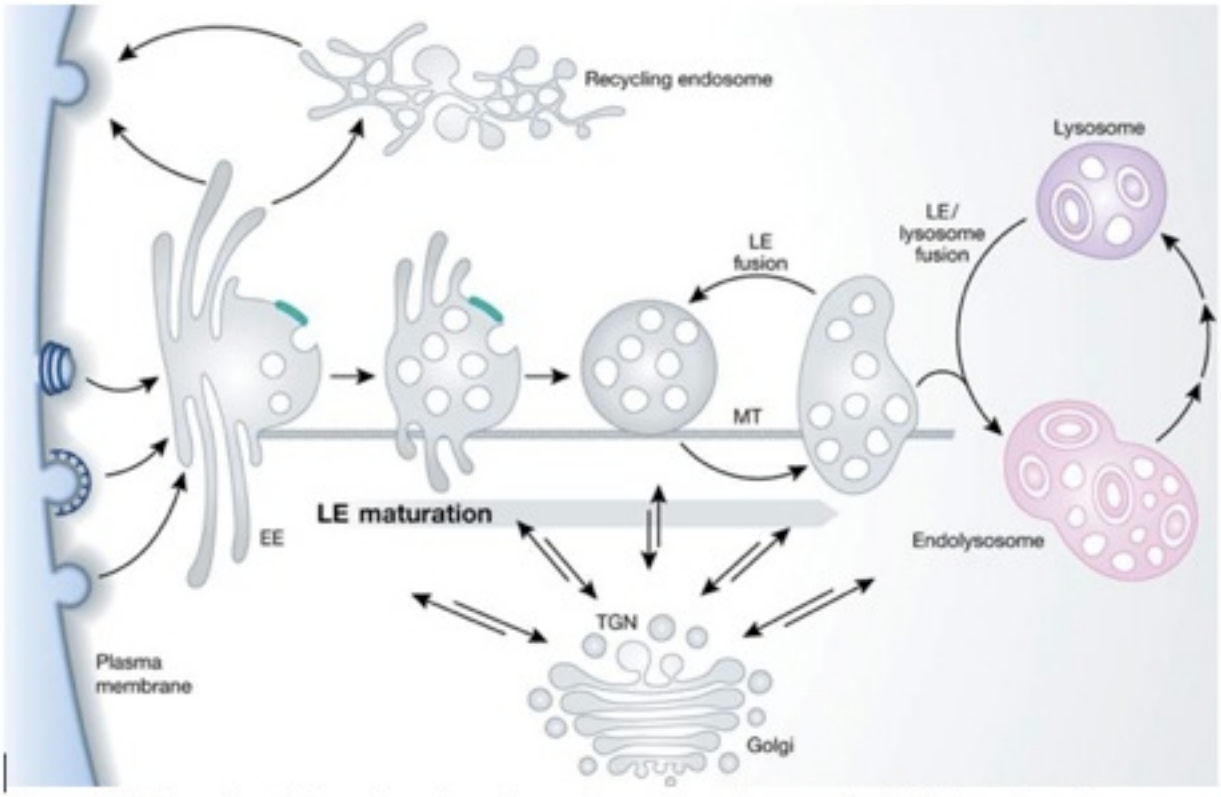

Figure 2: Schematic of the endocytic pathway. As early endosomes bud off from the plasma membrane, they mature to ILV-containing late endosomes (MVBs). Eventual fusion with the lysosome, or vacuole in yeast, is the last step and allows for degradation of their lumenal contents. Figure from Huotari and Helenius, 2011.

The process of MVB biogenesis and protein degradation is conserved across all eukaryotes, and is orchestrated by a fascinating class of proteins deemed the endosomal sorting complexes required for transport, or simply ESCRTs (Babst, 2005). Also implicated in retroviral budding and the final scission step in cytokinesis, the ESCRT machinery is composed of four sequential heteromeric protein complexes, starting with ESCRT-0 and ending with ESCRT-III. First, a target protein is ubiquitinated on its cytosolic surface and endocytosed via the clathrin

complex to form an early endosome within the cell. At this juncture, proteins destined for recycling are returned to their site of action, while proteins marked for degradation are recognized as such by ESCRT-0. ESCRT-0 is recruited to the endosome surface via its binding to the endosomal membrane phospholipid phosphatidylinositol 3-phosphate (PtdIns-3-P), and is thought to help concentrate the protein cargo (Teis et al., 2010). Next, the ESCRT-I complex binds to the ubiquitinated endosomal cargo, which in turn activates and recruits ESCRT-II to the action site. The recruitment of both ESCRT-I and ESCRT-II is concentrated to the neck of the forming invagination, and together are thought to ultimately deform the endosomal membrane and induce ILV budding into the lumen (Hurley & Hanson, 2010). At last, the catalysis of the final scission event of the ILV into the lumen of the endosome is accomplished via ESCRT-III. In this process, Vps25 of ESCRT-II recruits Vps20, the vanguard of ESCRT-III, to the forming invagination. Vps20 nucleates the homo-oligomerization of the the most prevalent ESCRT-III component Snf7, whose assembly and subsequent capping by Vps24 effectively “pinches” off the budding vesicle into the lumen (Wollert et al., 2009). In addition to terminating Snf7 assembly, Vps24 then activates and associates with Vps2 (CHMP2B), the mutated protein in FTD3. At last, Vps2 recruits the AAATPase Vps4, which through the hydrolysis of ATP catalyzes the disassembly of the entire ESCRT complex, liberating all components for subsequent rounds of protein trafficking.

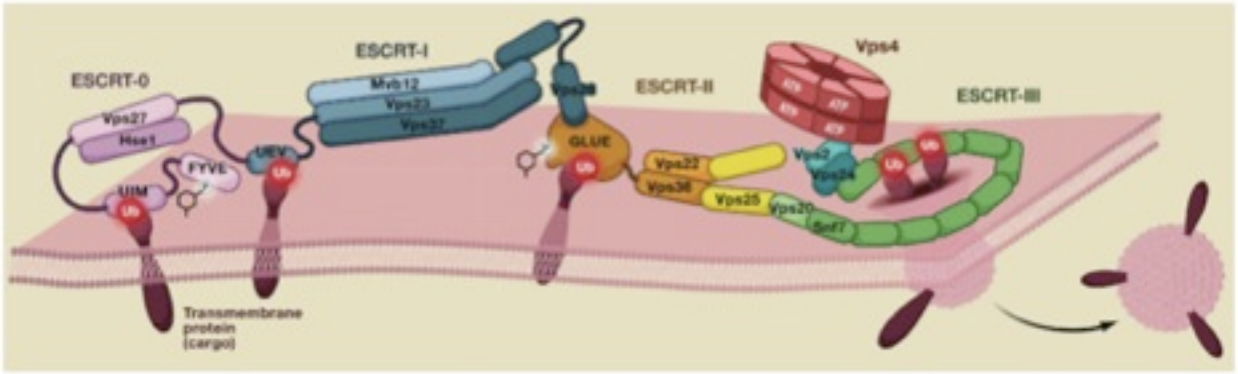

Figure 3: The fully assembled ESCRT machinery at the endosome membrane. ESCRT-III is the last heteromeric complex to be recruited, and initiates the scission of the forming ILV into the endosome lumen. AATPase Vps4, while not a constituent of ESCRT-III, is required for ESCRT disassembly mediated through the hydrolysis of ATP. Figure from Teis, 2009.

Current Data on Vps2ΔFTD3 and Project Aim

Ultimately, by integrating what is known about the ESCRT mediated endocytic pathway, the specific mutation of Vps2 in FTD3 (Vps2ΔFTD3), and recently acquired experimental data, this exposition details an investigation into the mechanistic basis for chromosome-3 linked frontotemporal dementia. In truncating the last 36 amino acids of Vps2, Vps2ΔFTD3 results in the elimination of two key protein motifs necessary for ESCRT-III function. All ESCRT-III proteins in their wild-type form include a conserved negatively-charged autoinhibitory domain at their respective carboxy-termini (Wollert et al., 2009). This domain enables the ESCRT-III components to exist as soluble cytosolic monomers when not assembled to budding endosomal membrane. In Vps2ΔFTD3, this auto-inhibitory domain is eliminated, and recent studies have indicated that afflicted cells showcase hyperactive Vps2ΔFTD3 assembly at the endosome membrane (Lee). Additionally, Vps2 utilizes a MIT interacting motif (MIM1) along its C-terminus in its interaction with Vps4 and its inherent microtubule interacting and transport (MIT) domain (Teis et al., 2009). Consequently, Vps2 is responsible for the recruitment and stimulation of Vps4, which via AATPase activity, allows for the disassembly of the ESCRT-III complex and

ensures subunit availability for subsequent rounds of protein degradation. The Vps2ΔFTD3 mutation omits the MIM1 region of Vps2, therefore eliminating its ability to recruit Vps4.

Recently, researcher Ian Smith in the Odorizzi laboratory examined the effects of Vps2ΔFTD3 using electron tomography and fluorescent microscopy, investigating the mutation's ramifications in both haploid (Vps2ΔFTD3) and heterozygous diploid (VPS2/FTD3) genotypes. In wild-type cells, electron tomography reveals cells with functional MVBs complete with distinct ILV's, often times in close proximity to their ultimate destination of the vacuole. In cells with an ESCRT-III null mutation, functional MVB's are replaced with aberrant endosomal structures known as class E-compartments. These abnormal formations take on a characteristic cisternal-like appearance and are the morphological hallmark of ESCRT-III dysfunction. Ian's electron microscopy data revealed that in haploid cells, the expression of a single mutated allele of Vps2ΔFTD3 results in the formation of E-compartments, a phenocopy of an ESCRT-III null mutation. While heterozygous cells expressing only one copy of Vps2ΔFTD3 exhibited MVB's and the absence of E-compartments, tomographs suggestive of a delay in ILV budding provide further evidence of an ESCRT implicated dysfunction. Next, fluorescent microscopy was employed to examine Vps2ΔFTD3's effect on protein localization and cargo sorting. As early endosomes mature to late endosomes and cargo is facilitated into ILVs, the initial membrane constituent Rab GTPase, Rab5, is exchanged for its predecessor, Rab7. This conversion, represented by the transfer of Vps21 for Ypt7 in yeast, serves as a unique marker for endosome maturation, and is necessary for efficient fusion with the vacuole (Russell et al., 2006). When both Rab GTPases were tagged with GFP and monitored for localization in heterozygous VPS2/FTD3 cells, both exhibited regular sorting. However, a heterozygous background did alter the

sorting of carboxypeptidase S (CPS), a transmembrane protein normally delivered to the vacuole for degradation. Vps2/FTD3 cells caused an accumulation of GFP marked puncta along the periphery the vacuole, indicative of abnormal late endosome accumulation. This data suggests a delay of some sort in endosome-lysosome fusion, and a potential consequence of the VPS2/ FTD3 background.

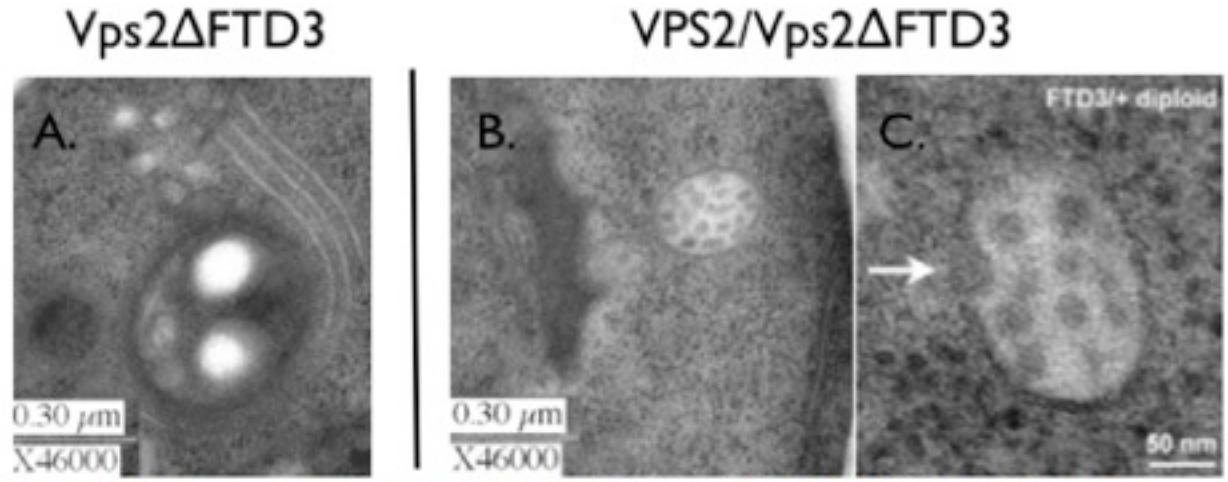

Figure 4: Electron tomographs examining Vps2ΔFTD3. A.) Haploid Vps2ΔFTD3 showcases aberrant E-compartment endosomal morphology. B.) Heterozygous diploid Vps2/FTD3 exhibits health MVBs. C. Putative forming invagination, suggestive of a delay in ILV budding. Unpublished Odorizzi lab data.

Finally, data from other labs has supported our findings thus far, and has implicated a new potential malfunctioning pathway in FTD3, autophagy. In examining both mammalian cell models and *Drosophila melanogaster,* recent studies report that an ectopic overexpression of aberrant Vps2ΔFTD3 results in the abnormal accumulation of both late endosomes (MVBs) and autophagosomes (Filimonenko et al., 2007, Lee et al., 2007). This information suggests that Vps2ΔFTD3 may hinder autophagic processing. Similar to endosome mediated protein degradation, autophagy provides a mechanism for the breakdown of cytosolic contents and organelles, and is heavily implicated in cellular response to stress and starvation conditions (Yang & Klionsky, 2010). Importantly, an impairment of autophagy results in neurodegeneration

in mice (Urwin et al., 2009), and its study hold promise in understanding human neurodegenerative disease. Its implication in FTD3 suggests a promising avenue in frontotemporal dementia research.

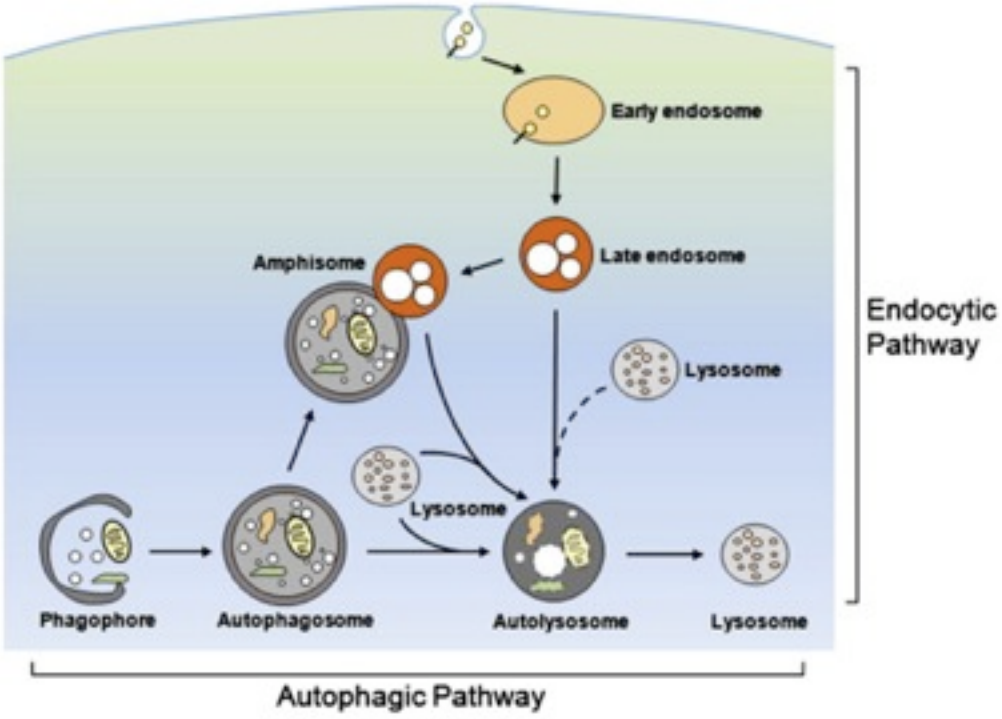

Figure 5: Representation of the autophagic pathway, a mechanism for the degradation of cytosolic proteins and organelles. The formation of an initial phagohore gives way to a fully-formed, double-membraned autophagosome. The autophagosome may be directly trafficked to the lysosome, or may overlap with the endocytic pathway and form an amphisome before fusion with the lysosome. Figure from Nixon and Yang, 2011.

Materials and Methods

Yeast Strain Construction

The standard utilization of PCR-based gene deletion cassettes was used in the construction in all Vps2ΔFTD3 strains, as well as autophagy mutant strains. Ploidy of diploid strains was confirmed via halo assay. Wild-type and vps4Δ controls were restreaked from -80˚C onto standard YPD agar plates.

Autophagic Flux Assay:

All assayed strains were transformed with a regular expression GFP-Atg8 plasmid (SLS5916), and plated on selectable marker -URA plates. Transformants were then grown in YNB-URA at 30˚C to saturation overnight. Saturated cultures were cut back to .20 ODU and allowed to grow for 1.5 hours. Next, strains designated for autophagy induction were treated with rapamycin at a concentration of .2ug/ml, and all strains were allowed to incubate for an additional three hours. Following incubation, cells were collected, subject to glass bead lysis, and TCA precipitated. Protein samples were resuspended in 1X SDS-PAGE sample buffer +.2% BME, and .5 OD600 units were resolved on large 12% SDS-polyacrylimide gels. Protein transfer to nitrocellulose membrane was done overnight, and resulting membrane was blocked for 1.5 hours in 10% milk/TBST. Primary mouse anti-GFP antibody was administered at a 1:2000 dilution overnight. Following three five minute washes with .05% TBST, mouse specific HRP-conjugated secondary was applied for 3 hours. Two more TBST washes followed by a final TBS wash prepared the membrane for chemiluminescent visualization on x-ray film. An X-ray exposure time of 45 minutes was implemented.

Snf7 Polymerization Assay:

Before cellular lysates were harvested, the linear glycerol gradients were prepared. 10%, 20%, 30% and 40% stocks of glycerol were made up in PBS +.5% Tween 20. A separate gradient was poured concurrently for each cell strain. First, 2.5 mls of 40% glycerol was pipetted into a test tube. Very slowly, 2.5 mls of the 30% glycerol was layered on top, followed by 2 mls of the 20% glycerol. Next, a mixture of the 10% glycerol/lysis buffer/1% Triton X-100/PIC solution topped the gradient. To convert the gradients from step to linear gradients, a pre-spin at 30,000 rpm for one hour was done.

All examined strains were grown to saturation overnight in YPD, and cut back to .20 ODU in 50 ml of the same media. Once cells reached mid-logarithmic growth phase they were harvested, washed, spheroplasted and dounced. Unbroken cells were removed following a 3 minute spin at 3000 rpm. The P13 fragment was solubilized in 1-ml of PBS+0.5% Tween, and passed through a 25G5/8 needle five times before a 10 minute spin at 13000 rpm. Finally the supernatant, corresponding to 30 OD600 units of each cell strain, was delicately loaded on top of the ready glycerol gradients. Each loaded gradient was subject to a 4 hour 100000 x g centrifugation at 4˚C. Upon completion of centrifugation, 11 distinct 1-ml fractions were collected from each gradient run, with the first fraction corresponding to lowest glycerol density. Each fractionation was subject to TCA protein precipitation, with each pellet resuspended via sonication in 1X SDS-PAGE sample buffer +.2% BME. In total, 25 ul of each fractionation was loaded in descending order onto a 10% SDS-polyacrylimide gel. Subsequent western blot protocol mirrors the procedure previously described in "Autophagy Flux Assay" with the following exceptions. Snf7 antisera was used as the primary antibody, and rabbit specific HRP-conjugated secondary was applied. Additionally, an x-ray exposure time of 15 minutes was sufficient for detection.

Size standards for the 10%–40% glycerol gradient were previously established by graduate student Natalie Johnson by examining the localization of aldolase (156 kD), catalase (232 kD), ferritin (440 kD) and thyroglobulin (670 kD). Wild-type and Vps4Δ polymerization results were supplied by Natalie Johnson and allowed for insight into the assembly pattern of healthy and ESCRT-III dysfunctional cells.

Results

Autophagic processing of GFP-Atg8 is unaffected in Vps2ΔFTD3 mutants

As recent data reports a marked accumulation of autophagosomes as a consequence of ectopic over-expression of mutated Vps2ΔFTD3, the autophagic pathway represents a key target for research. In order to investigate Vps2FTD3's potential effects on the autophagic process, an experiment monitoring the processing of the chimeric protein GFP-Atg8 was conducted. Upon the induction of autophagy, the ubiquitin-like autophagy-related protein 8 (Atg8) becomes tightly associated with the inner vesicle of the double membraned autophagosome, where it is ultimately transported to the vacuole for degradation (Xie et al., 2008). Fortunately, tagging the amino terminus of Atg8 with green fluorescent protein (GFP) offers a convenient way for analyzing autophagy. The GFP tag does not interfere with Atg8 localization, and the chimeric version is similarly brought to the vacuole for degradation. In contrast to Atg8, GFP is relatively resistant to proteolysis and is released from Atg8 as free GFP in the vacoule. Consequently, the appearance of free GFP and its corresponding molecular weight can be detected via western blot and compared to levels of non-processed chimera (Tomohiro Yorimitsu et al., 2009).

Seven different yeast strains and subsequent genotypes were monitored for autophagy processing. Three of the strains were subjected to PCR-mediated gene deletion of the protein Atg1. The deletion of Atg1 effectively blocks the induction of autophagy and provides bona-fide examples of non-functional mutants for the autophagic pathway (T Yorimitsu & Klionsky, 2005). The inclusion of two wild-type strains, one haploid and one diploid, allows for an observable control. Of primary focus was the haploid and diploid mutants expressing truncated Vps2ΔFTD3. Following their creation and confirmation of their respective genetic background,

all strains were transformed with a regular copy plasmid expressing GFP-Atg8. Autophagy was induced via rapamycin treatment in each strain genotype, with a counterpart strain receiving no drug. Each culture was subject to trichloroacetic acid (TCA) protein precipitation, resolved via SDS-PAGE, and probed for GFP using standard western blot protocol.

Ultimately, both wild-type haploid and diploid yeast strains showcased processing of the chimeric GFP-Atg8 protein. Rapamycin treatment and consequent autophagy induction increased visible free GFP in both backgrounds, but was also accompanied by a basal, albeit reduced, level of autophagy in untreated counterparts. As expected, all Atg1 knockout strains exhibited a complete inability to undergo autophagy, and no free GFP was detected. This result was also replicated in a strain heterozygous for the FTD3 truncation with accompanying homozygous Atg1 knockouts. Finally, haploid Vps2ΔFTD3 showcased results similar to wild-type controls, with autophagy occurring in both the uninduced and rapamycin treated strains, with a slight increase observed in the latter. The heterozygous strain for the FTD3 mutation did not exhibit impaired autophagy, and free GFP was detected following treatment with rapamycin. Non-treated heterozygous VPS2/Vps2ΔFTD3 did not show free GFP detectable via western blot, an observation unique in the context of functional Atg1.

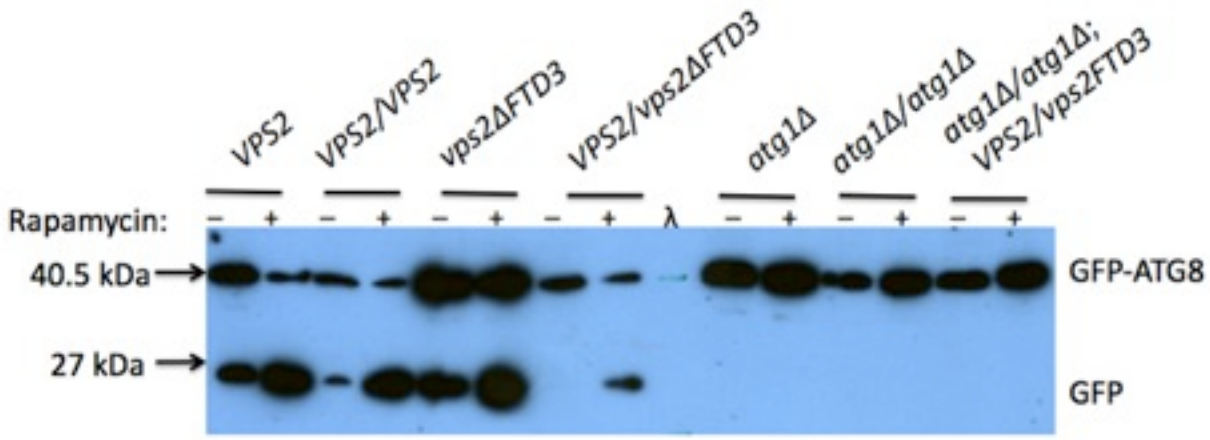

Figure 6: Autophagic flux assay. The processing of chimeric GFP-Atg8 was monitored by the appearance of free GFP via western blot. Autophagy is not inhibited in either haploid vps2ΔFTD3 or heterozygous diploid VPS2/vps2ΔFTD3.

Snf7 polymerization is affected in haploid, but not diploid Vps2ΔFTD3 mutants

Vps2 represents an essential component in the function of the ESCRT-III complex on late endosomes. Wild-type Vps2 functions in conjunction with Vps20 to cap and terminate the homooligomerization of Snf7, the main driver of ILV scission into the endosome. Vps2 additionally recruits and stimulates the AATpase Vps4, which in turn catalyzes the dissociation of the ESCRT-III complex. As a result, a sizing analysis assay was performed in order to monitor potential effects of Vps2ΔFTD3 on the polymerization of Snf7. Both haploid and heterozygous diploid strains for Vps2ΔFTD3 were examined, in conjunction with a wild-type diploid control. Unpublished data from Odorizzi laboratory graduate student Natalie Johnson was employed to validate experimental wild-type controls, establish protein size standards, as well provide a comparative example of aberrant Snf7 polymerization as exhibited in a Vps4Δ strain.

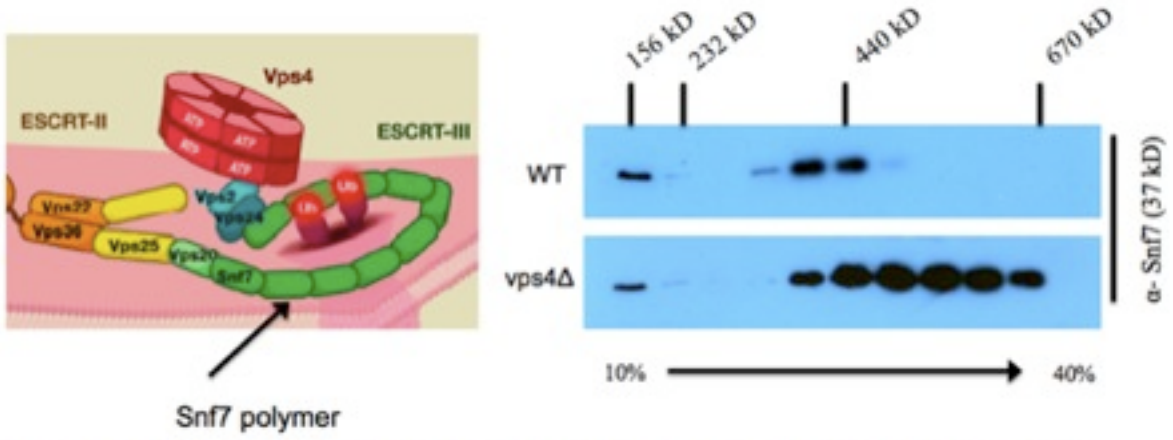

Figure 7: Established controls for Snf7 polymerization experiment. Wild-type cells exhibit distinct monomer and polymer regions via western blot. Vps4Δ represents a genotype unable to disassemble the ESCRTs, resulting in a Snf7 concentration at a denser fractionation.

In order to conduct the experiment, cultures of all three strains were harvested, spheroplasted, and subjected to sub-cellular fractionation to enrich for membranes. The solubilized membrane fractions (P13) were then subject to a 10%–40% glycerol velocity sedimentation gradient. 11 different size fractionations were harvested from each cell strain, trichloroacetic acid (TCA) precipitated, resolved via SDS-PAGE, and probed with Snf7 specific antisera. The distribution of Snf7 along the density gradient was examined in order to ascertain potential effects of the FTD3 mutation.

Consistent with established control data from the lab, the wild-type diploid strain showcased two distinct populations of Snf7 at endosomes, corresponding to both a monomer and polymer population. At approximately the 156 kilodaltons (kD) fraction, a robust band was resolved as representative of the Snf7 monomer at the first fraction on the gradient. A characteristic Snf7 polymer was found distributed at a higher density region, corresponding to a heavier molecular weight. In contrast, the haploid strain expressing Vps2FTD3 showcased some level of Snf7 detection in each of the 11 fractions. Two regions of noticeable Snf7 concentration

occurred at approximately 232kD, as well as the terminal two fractions of the gradient. These two regions of increased Snf7 accumulation may correspond to the monomer and polymer of Snf7 assembly. An increased Snf7 detection at the higher density fractions resembles the detection assay characteristic of a Vps4 knockout strain. Vps4Δ strains lack the ability to dissociated the ESCRT-III complex, and remain constituently assembled. Finally, heterozygous VPS2/Vps2ΔFTD3 exhibited a Snf7 polymerization pattern similar to the wild-type control. A clear monomeric accumulation of Snf7 was shown in the lowest density fraction taken, and supplemented by an inferred polymeric complex at a separate, denser section of the blot. No other regions of the VPS2/Vps2ΔFTD3 blot presented evidence of Snf7 accumulation.

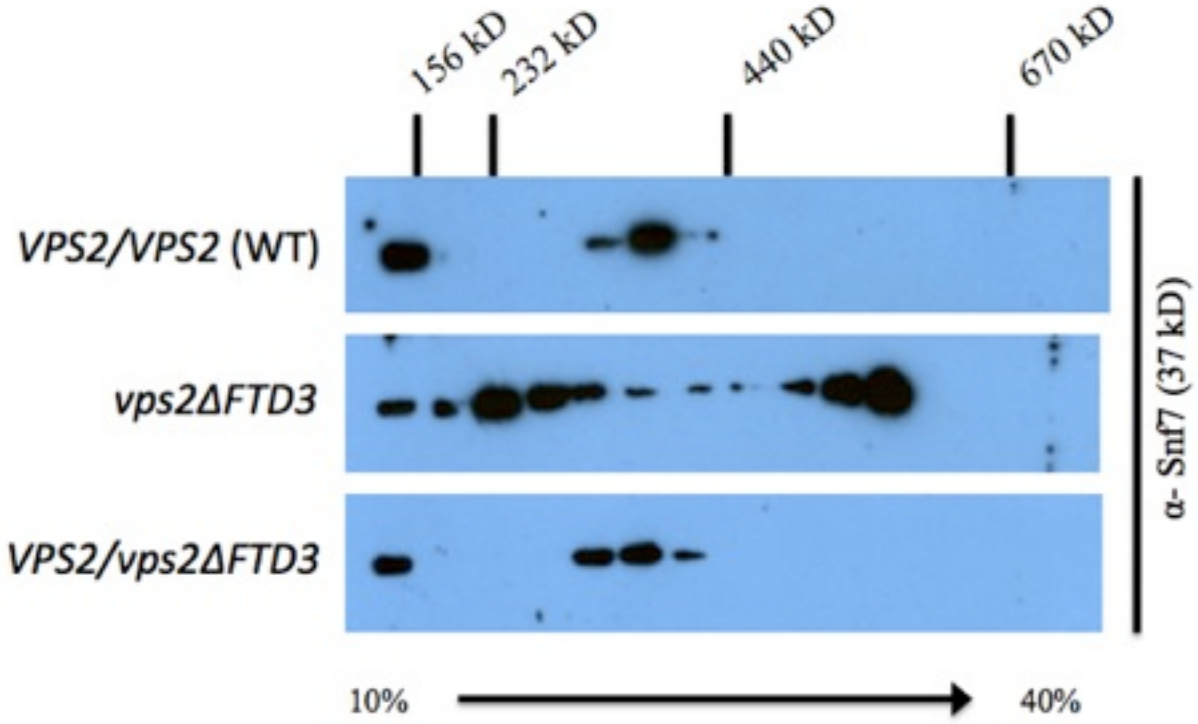

Figure 8: Snf7 polymerization experiment. Haploid vps2ΔFTD3 showcases abnormal Snf7 polymerization, detectable across varied molecular weights. Heterozygous VPS2/Vps2ΔFTD3 presents Snf7 polymerization parallel to wild-type controls, with a single distinct monomeric region and separate heavier polymer region.

Discussion

Vps2ΔFTD3 and Autophagy

The mutation of Vps2 involved in chromosome 3-linked frontotemporal dementia (FTD3) implicates a variety of different cellular processes as potential causes of the neurodegenerative disease. One such cellular mechanism, the autophagic pathway, has recently been suggested as a prospective cause for the pathology described in humans. Autophagy serves as the predominant method of bulk degradation for organelles and soluble cytosolic proteins, and is highly conserved amongst eukaryotes. This process is facilitated by the formation of the double membraned autophagosome, which sequesters cargo within its internal vesicular lumen and is trafficked to the vacuole for degradation. The autophagosome may be transported directly to the vacuole, or alternatively, the autophagosome may fuse with a mature late endosome, forming a hybrid amphisome, which is then transported to the vacuole (Figure 5) (T Yorimitsu & Klionsky, 2005). Defects in autophagy have been linked to a variety of neurodegenerative diseases, including Alzheimer's, Huntington's, and Parkinson's disease (Rusten & Stenmark, 2009). These pathologies are hypothesized to result from an insufficient degradative clearing of proteins, resulting in detrimental aggregation in afflicted neurons.

In the case of FTD3, ectopic over-expression of Vps2ΔFTD3 results in a marked accumulation of autophagosomes and late endosomes in mammalian and fly cell models. Importantly, this phenotype is replicated in ESCRT-depleted cells, and consequently leads to the hypothesis that not only are the ESCRTs required for efficient autophagy, but also that mutated Vps2ΔFTD3 may be responsible for aberrant autophagy in FTD3. Specifically, the increased number of autophagosomes could be a consequence of decreased autophagic processing. In order

to test this theory, autophagic flux was assayed in haploid and FTD3 heterozygous mutants. Autophagy response was compared alongside bone-fide autophagy mutants incapable of initiating autophagy, as well as wild-type controls. Should expression of Vps2ΔFTD3 affect the pathway, its western blot detection would closer resemble the autophagy mutants than wild-type controls.

Ultimately, our results indicate expression of either haploid or heterozygous diploid Vps2ΔFTD3 does not significantly effect rapamycin-induced autophagic processing of chimeric GFP-Atg8. This experiment was repeated in triplicate, with each trial yielding parallel results. In the context of functional Atg1, autophagy was successfully induced, and free GFP was detected in all pertinent strains. In contrast, all functional knockouts of Atg1 resulted in no free GFP, consistent with Atg1's irreplaceable role in autophagy initiation.

While our results indicate that Vps2ΔFTD3 does not cause a decrease in autophagic processing, and consequently is not a substantiated cause of observed autophagosome accumulation, other alternative explanations exist. For example, aberrant autophagosome accumulation may be the result of enhanced initiation of the autophagic pathway, as opposed to faulty autophagosome-vacuole fusion. It is important to note that the relationship between ESCRTs and the autophagic pathway is only beginning to be investigated, and their association with one another is still unclear. Subsequently, the mutation in Vps2ΔFTD3 may directly affect only the ESCRTs, yet in turn have an indirect effect on autophagy. With faulty endocytic cargo trafficking in the ESCRT mediated endocytic pathway, unknown intracellular signals may result in an increase in autophagy, executed in a 'rescue-attempt' to compensate for deficient protein trafficking. Such a response could logically cause an up-regulation in autophagosome formation,

and likely result in the observed phenotype. Additionally, the Vps2ΔFTD3 mutation may ultimately affect the bioavailability of specific nutrients needed for regular cell function, as ESCRTs aid in the regulation of transmembrane receptors at the cell surface, such as the transferrin receptor. Aberrant Vps2ΔFTD3 could ultimately result in a response associated with inefficient nutrients, which is a well-characterized initiator of autophagy. In turn, an up-regulation of autophagosomes could result in an increase in protein degradation and subsequently combat starvation. Needless to say, additional studies are needed in order to fully resolve Vps2ΔFTD3's role in autophagy.

Vps2ΔFTD3 and Snf7 Polymerization

Principle amongst its functions, Vps2 represents a well-characterized constituent of the ESCRT-regulated endocytic pathway. A member of the final heteromeric ESCRT-III complex, it functions in two well-known roles. First, following vesicular bud formation, it associates with Vps24 to form a capping mechanism that terminates the oligomerization of Snf7, a process credited for catalyzing ILV scission into the late endosome. It then subsequently utilizes its MIM1 domain to bind the MIT portion of Vps4. This protein-protein interaction galvanizes the AATpase activity of Vps4, and the hydrolysis of ATP results in the disassembly of the ESCRT-III polymer allowing for future rounds of ILV scission. As such, the mutation of Vps2 in chromosome-3 linked frontotemporal dementia has yielded strong evidence to support the hypothesis that it causes dysfunction in the endocytic process.

Unpublished fluorescent microscopy and electron tomography data from the Odorizzi lab has implicated protein missorting, aberrant vesicle morphology, and a potential delay in ILV budding resulting from Vps2FTD3. Outside data affirms these observations, reporting that the

ectopic over-expression of Vps2ΔFTD3 leads to an abnormal accumulation of late endosomes at the vacuole periphery. This information leads to the hypothesis that Vps2ΔFTD3 may interfere with the polymerization or ultimate disassembly of the Snf7 oligomer. Of all the ESCRT-III proteins, Snf7 is the only one shown to be absolutely imperative in ILV severing, a process which data suggests is delayed in FTD3. Additionally, the truncation in Vps2ΔFTD3 removes its MIM1 domain, which is necessary in the enlistment of Vps4. Without Vps4, Snf7 and the entire ESCRT-III complex becomes trapped as an assembled complex at the endosome membrane (Wemmer et al., 2011). Ultimately, a Snf7 specific sizing assay was performed in order to test how Vps2ΔFTD3 affects the polymerization of Snf7.

Overall, our results indicate that haploid Vps2ΔFTD3 produces abnormal Snf7 polymerization, while in contrast heterozygous VPS2/Vps2ΔFTD3 cells exhibit healthy Snf7 polymerization consistent with wild-type cells. In the case of the heterozygous diploid and wild-type controls, a clear Snf7 monomer at the lowest density fractionation suggests monomeric Snf7 is recruited and available for assembly as needed to form ILVs. Higher density fractions represent the transient polymer present in a wild-type context. As for haploid Vps2ΔFTD3, Snf7 assembly is showcased at every probed molecular weight level. Two regions of increased Snf7 detection, one region above and the other below the transient wild-type polymer, indicate some level of Snf7 polymer formation, but both differ from wild-type in their size. Additionally, when compared to a nonfunctional Vps4 blot in which ESCRT-III is unable to disassemble, both exhibit marked detection at the highest density fractions. This is suggestive that the truncation in some part enhances the formation or hinders the release of Snf7. At the time of this exposition,

this experiment has been conducted though its first trial, and additional trials will further elucidate Vps2FTD3's effect on Snf7 oligomerization.

Altogether, Vps2ΔFTD3 does seem to effect Snf7 polymerization when a truncated version represents the sole expressed form. This finding is in accordance with electron tomography images, which showcase haploid cells with aberrant E-compartments in place of healthy MVB's. However, as heterozygous expression does not seem to alter Snf7 activity, it seems unlikely that this mechanism alone can account for the pathology seen in humans. As the Vps2ΔFTD3 mutation removes both its innate auto-inhibitory regions and protein interaction domains, a variety of assays are required to distinguish the exact mechanism of pathology.

Future Direction

When considered together, the autophagy and Snf7 polymerization assays of this study suggest that the central pathology behind FTD3 remains unclear. Autophagic flux as monitored by the cleavage of chimeric marker GFP-Atg8 does not appear altered in haploid or heterozygous diploid strains expressing Vps2ΔFTD3. Additionally, altered polymerization of Snf7 is observed in haploid Vps2ΔFTD3, yet diploid VPS2/Vps2ΔFTD3 seems sufficient in maintaining a healthy assembly pattern. These results provide inspiration for a new complement of experiments, which should help further resolve the mechanism underlying FTD3. In terms of monitoring autophagy, the next step is to employ fluorescent microscopy to examine the localization of GFP-Atg8 in Vps2ΔFTD3 afflicted, autophagic cells. Upon rapamycin-induced autophagy, previous studies have found GFP-Atg8 to localize to the vacuole, a process facilitated by either autophagosome-endosome fusion or direct autophagosome-vacoule fusion. A mislocalization of GFP-Atg8 in Vps2ΔFTD3 would provide supporting evidence of a defect in the autophagic pathway, and a

potential contributing cause behind FTD3. Pertaining to the Snf7 polymerization assay, additional trials should be repeated in order to confirm our initial findings. Auxiliary experiments are also necessary in order to pinpoint other potential malfunctioning ESCRT-III subunit interactions. To accomplish this, in vivo native immunoprecipitation or in vitro pulldown assays can be implemented to discern both wild type and mutated Vps2ΔFTD3's binding partners. Differing protein interactions or expression levels in FTD3 afflicted cells would provide new evidence for altered ESCRT-III activity as the mechanism for pathology. Finally, more work investigating the potential for a malfunctioning Rab GTPase conversion event must be done. As endosomes mature from early endosomes to ILV-containing late endosomes (MVBs), the membrane constituent Rab5 is exchanged for its predecessor Rab7. Rab7, in addition to serving as an endosome maturity marker, is required for both endosome and autophagosome fusion with the vacuole. Despite preliminary fluorescent microscopy evidence that heterozygous Vps2ΔFTD3 does not change localization of either Rab, this key pathway remains a likely target for dysfunction in FTD3. As such, sample lysates have already been prepped for work with Odorizzi lab collaborator Dr. Alex Merz at the University of Washington, who will investigate the biochemical status of Rab5 and Rab7 in FTD3 impaired cells.

Finally, the findings detailed in this thesis, accompanied by future prospective experiments, should provide key insight behind Vps2ΔFTD3's effect on cell function. Autophagy, ESCRT-III interactions, and Rab conversion with their potential malfunction all present intriguing projects in the investigation of the FTD3 mutation. Ultimately, further scientific examination should yield new understanding into both the basic science of Vps2 and the ESCRTs, as well as the mechanism behind frontotemporal dementia linked to chromosome 3.

References

Babst, M. (2005). A protein's final ESCRT. *Traffic (Copenhagen, Denmark)*, *6*(1), 2–9. doi: 10.1111/j.1600-0854.2004.00246.x

Filimonenko, M., Stuffers, S., Raiborg, C., Yamamoto, A., Malerød, L., Fisher, E. M. C., Simonsen, A. (2007). Functional multivesicular bodies are required for autophagic clearance of protein aggregates associated with neurodegenerative disease. *The Journal of Cell Biology*, *179*(3), 485–500. doi:10.1083/jcb.200702115

Hodges, J. R. (2001). Frontotemporal dementia (Pick's disease): clinical features and assessment. *Neurology*, *56*(11 Suppl 4), S6–10.

Huotari, J., & Helenius, A. (2011). Endosome maturation. *The EMBO Journal*, *30*(17), 3481–3500. doi:10.1038/emboj.2011.286

Hurley, J. H., & Hanson, P. I. (2010). Membrane budding and scission by the ESCRT machinery: it's all in the neck. *Nature Reviews Molecular Cell Biology*, *11*(8), 556–566. doi:10.1038/nrm2937

Isaacs, A. M., Johannsen, P., Holm, I., & Nielsen, J. E. (2011). Frontotemporal dementia caused by CHMP2B mutations. *Current Alzheimer research*, *8*(3), 246–251.

Lee, J.-A., Beigneux, A., Ahmad, S. T., Young, S. G., & Gao, F.-B. (2007). ESCRT-III dysfunction causes autophagosome accumulation and neurodegeneration. *Current biology: CB*, *17*(18), 1561–1567. doi:10.1016/j.cub.2007.07.029

Mackenzie, I. R. A., Baker, M., Pickering-Brown, S., Hsiung, G.-Y. R., Lindholm, C., Dwosh, E., … Feldman, H. H. (2006). The neuropathology of frontotemporal lobar degeneration

caused by mutations in the progranulin gene. *Brain: a journal of neurology*, *129*(Pt 11), 3081–3090. doi:10.1093/brain/awl271

Nixon, R. A., & Yang, D.-S. (2011). Autophagy failure in Alzheimer's disease--locating the primary defect. *Neurobiology of disease*, *43*(1), 38–45. doi:10.1016/j.nbd.2011.01.021

Raiborg, C., & Stenmark, H. (2009). The ESCRT machinery in endosomal sorting of ubiquitylated membrane proteins. *Nature*, *458*(7237), 445–452. doi:10.1038/nature07961

Russell, M. R. G., Nickerson, D. P., & Odorizzi, G. (2006). Molecular mechanisms of late endosome morphology, identity and sorting. *Current Opinion in Cell Biology*, *18*(4), 422–428. doi:10.1016/j.ceb.2006.06.002

Rusten, T. E., & Stenmark, H. (2009). How do ESCRT proteins control autophagy? *Journal of cell science*, *122*(Pt 13), 2179–2183. doi:10.1242/jcs.050021

Seelaar, H., Rohrer, J. D., Pijnenburg, Y. A. L., Fox, N. C., & Van Swieten, J. C. (2011). Clinical, genetic and pathological heterogeneity of frontotemporal dementia: a review. *Journal of neurology, neurosurgery, and psychiatry*, *82*(5), 476–486. doi:10.1136/jnnp.2010.212225

Skibinski, G., Parkinson, N. J., Brown, J. M., Chakrabarti, L., Lloyd, S. L., Hummerich, H., … Collinge, J. (2005). Mutations in the endosomal ESCRTIII-complex subunit CHMP2B in frontotemporal dementia. *Nature Genetics*, *37*(8), 806–808. doi:10.1038/ng1609

Snowden, J. S., Pickering-Brown, S. M., Mackenzie, I. R., Richardson, A. M. T., Varma, A., Neary, D., & Mann, D. M. A. (2006). Progranulin gene mutations associated with frontotemporal dementia and progressive non-fluent aphasia. *Brain: a journal of neurology*, *129*(Pt 11), 3091–3102. doi:10.1093/brain/awl267

Talbot, K., & Ansorge, O. (2006). Recent advances in the genetics of amyotrophic lateral sclerosis and frontotemporal dementia: common pathways in neurodegenerative disease. *Human Molecular Genetics*, *15*(suppl 2), R182–R187. doi:10.1093/hmg/ddl202

Teis, D., Saksena, S., & Emr, S. D. (2009). SnapShot: the ESCRT machinery. *Cell*, *137*(1), 182–182.e1. doi:10.1016/j.cell.2009.03.027

Teis, D., Saksena, S., Judson, B. L., & Emr, S. D. (2010). ESCRT-II coordinates the assembly of ESCRT-III filaments for cargo sorting and multivesicular body vesicle formation. *The EMBO journal*, *29*(5), 871–883. doi:10.1038/emboj.2009.408

Urwin, H., Ghazi-Noori, S., Collinge, J., & Isaacs, A. (2009). The role of CHMP2B in frontotemporal dementia. *Biochemical Society transactions*, *37*(Pt 1), 208–212. doi: 10.1042/BST0370208

Van der Zee, J., Urwin, H., Engelborghs, S., Bruyland, M., Vandenberghe, R., Dermaut, B., … Van Broeckhoven, C. (2008). CHMP2B C-truncating mutations in frontotemporal lobar degeneration are associated with an aberrant endosomal phenotype in vitro. *Human molecular genetics*, *17*(2), 313–322. doi:10.1093/hmg/ddm309

Wemmer, M., Azmi, I., West, M., Davies, B., Katzmann, D., & Odorizzi, G. (2011). Bro1 binding to Snf7 regulates ESCRT-III membrane scission activity in yeast. *The Journal of cell biology*, *192*(2), 295–306. doi:10.1083/jcb.201007018

Wittenberg, D., Possin, K. L., Rascovsky, K., Rankin, K. P., Miller, B. L., & Kramer, J. H. (2008). The early neuropsychological and behavioral characteristics of frontotemporal dementia. *Neuropsychology review*, *18*(1), 91–102. doi:10.1007/s11065-008-9056-z

Wollert, T., Wunder, C., Lippincott-Schwartz, J., & Hurley, J. H. (2009). Membrane scission by the ESCRT-III complex. *Nature*, *458*(7235), 172–177. doi:10.1038/nature07836

Xie, Z., Nair, U., & Klionsky, D. J. (2008). Atg8 controls phagophore expansion during autophagosome formation. *Molecular biology of the cell*, *19*(8), 3290–3298. doi:10.1091/mbc.E07-12-1292

Yang, Z., & Klionsky, D. J. (2010). Eaten alive: a history of macroautophagy. *Nature Cell Biology*, *12*(9), 814–822. doi:10.1038/ncb0910-814

Yorimitsu, T, & Klionsky, D. (2005). Autophagy: molecular machinery for self-eating. *Cell death and differentiation*, *12*(Suppl 2), 1542–1552. doi:10.1038/sj.cdd.4401765

Yorimitsu, Tomohiro, He, C., Wang, K., & Klionsky, D. J. (2009). Tap42-associated protein phosphatase type 2A negatively regulates induction of autophagy. *Autophagy*, *5*(5), 616–624.